Orbital: The Electronic Journal of Chemistry
journal homepage: www.orbital.ufms.br
e-ISSN 1984-6428

| Vol 11 | | No. 1 | | January-March 2019 |

FULL PAPER

Glass Ionomer Cements Based in TiO_2 by Sol-gel Method

Thiago Ilipronti[a], Carolina K Clare[a], Graciele Berndt[a], Elvio Antônio de Campos[a], Maria Helena Vaz Fernandes[b] and Silvia Denofre de Campos[a]

[a]Center of Engineering and Exact Sciences, CECE; State University of Western Paraná, Campus de Toledo, 85903-000, Toledo, Brazil.
[b]Department Materials and Ceramic Engineering, CICECO; University of Aveiro, Campus Universitário de Santiago, 3810-193, Aveiro, Portugal.

Article history: Received: 19 June 2018; revised: 18 August 2018; accepted: 03 March 2019. Available online: 30 March 2019. DOI: http://dx.doi.org/10.17807/orbital.v11i1.1176

Abstract:

Glass ionomer cements are used in dentistry for applications such as luting cements and as restoratives materials, due to their ability to chemically bond to the tooth. The glasses used in the cements are based on calcium aluminum silicates and calcium fluoride. This study aimed at preparing a glass systems containing titanium oxide to be used in glass ionomer cements. Powders with the composition $47SiO_2$-13CaO-$29Na_2O$-$7P_2O_5$-$4TiO_2$ were synthesized by the sol-gel method, one prepared with TiO_2 powder (A1) and the other with titanium tetraisopropoxide (A2). The obtained powders exhibited a specific surface area of 83.63 m^2g^{-1} and 15.79 m^2g^{-1} and pore diameter of 42.07 Å and 90 Å for A1 and A2, respectively. The XRD results indicated that the material is partially crystalline with weak diffraction peaks related to titanium oxide (anatase). The FTIR and Raman spectroscopy analyses showed that SiO_4 tetrahedra are found in the same coordination both in the synthesized glasses network and in the commercial glass ionomer cements Vidrion C® Cementation and Maxion®R Restorative, used for comparative purposes. The introduction of Ti^{4+} ions in the powders developed in this work provided properties and the structural characteristics indicating their potential for applications as ionomer cements.

Keywords: ionomer cements; sol-gel; structural properties; thermal stability; titanium oxide

1. Introduction

The last decade has seen an increasing interest concerning the synthesis and applications of calcium phosphate glasses, especially for bone-related applications, like prosthesis coatings, filling materials, tissue engineering and cements for restorative dentistry. This is attributed to their bioactivity and potential resorption abilities due to the structural similarity with the mineral formulation of bones and teeth [1–3]. Glass ionomer cements present as the main advantage a remarkable capacity of binding to dentine and enamel through chemical reactions, a significant anticariogenic property due to the controlled release of fluoride, preserving a biological compatibility with a reduced cytotoxicity [4–8]. A typical glass ionomer cement is formed by a calcium aluminum fluorosilicate glass powder that reacts with a poly(organic acid) resulting in a composite paste that hardens with time [9–12]. These glasses are usually prepared at high temperatures by the melt-quenching method, which requires a tight process control in order to avoid the loss of fluoride and changes in the batch composition. A thermal treatment of the ionomer glass is usually performed to reduce the thermal stress induced by the quick cooling, but it can also be used to promote its crystallization. This treatment usually leads to an improvement of the mechanical properties and an increased chemical stability of the materials [13–16].

Various silicate and phosphorus-containing compositions have been prepared by the sol-gel process [17–21]. This preparation method has attracted the attention of the scientific community since the obtained materials are chemically homogeneous, have high purity, and require a

*Corresponding author. E-mail: silviadenofre@uol.com.br

synthesis temperature much lower than the one needed in the conventional method. It was observed that a sol-gel derived silica gel or titanium gel showed Si-OH and Ti-OH groups in abundance on their surface. It is believed that these groups are important reactive sites for bond interactions with bone tissues or adhesion to dental surfaces when used with glass ionomer cements [22]. These sites are also responsible for inducing apatite nucleation in bio-implant applications. Therefore, the presence of the components that induce the formation of these active sites when obtaining the material is very relevant in the bioactivity development. The higher the bioactivity of the material, the better is its adherence process. Some glass compositions, such as those based on calcium fluorosilicates, have been tested to obtain glass ionomer cements. The anticarciogenic properties of glass ionomer cements are derived from the fluoride component of the powder. The fluoride release from the restorative materials acts as a topical application, increasing the fluoride content around the tooth. Studies showed that the use of nanoparticles of TiO_2, CuO, ZnO, and Ag_2O incorporated to glass ionomer cements enhanced the micro hardness, strength and also contributed to the antibacterial activity of these materials.[23–26].

Previous studies have demonstrated that the SiO_2-CaO-Na_2O-P_2O_5 system can present a bioactive behavior. The incorporation of the titanium oxide to the composition can improve the mechanical properties and provide an antibacterial activity. Thus, the purpose of this work is to develop, by the sol-gel method, new compositions based on the SiO_2-CaO-Na_2O-P_2O_5 system, modified by the addition of titanium oxide in place of the fluoride, besides checking if different sources of TiO_2 might influence the physicochemical properties of the material when preparing dental cements.

2. Results and Discussion

The values of specific surface area (S_{BET}) of the powders synthesized using titanium oxide and titanium tetra-isopropoxide (compositions A1 and A2, respectively) after a jellification time of one week, are presented in Table 1.

Table 1. Textural parameters of the powders obtained by the sol-gel method from the system SiO_2-CaO-Na_2O-P_2O_5-TiO_2 (two different TiO_2 sources).

Sample	TiO_2 sources	Surface area (m^2/g)	Pore volume (cm^3/g)	Pore diameter (Å)	Calculated pore diameter* (Å)
A1	TiO_2 powder	83.63	0.086	42.07	41.25
A2	TTP	15.79	0.043	90.03	110.90
Maxxion R® Restorative	commercial	8.34	0.007	61.84	17.02
Vidrion C® Cementation	commercial	28,74	0.052	29.34	36.18

* Calculated pore diameter: $d = 2\,Vp/S_{BET;}$ where Vp = pore volume and $S_{BET=}$ specific surface area.

It was observed that sample A1 showed a specific surface area higher than sample A2, and the pore diameter of the sample A2 is about twice the one observed for sample A1 (Table 1).

The observed difference in the specific surface area of A1 and A2 samples may be related to the way in which the titanium oxide was introduced during the sample preparation. Some authors agree that, when all reactants are in the same phase, there is a more efficient contact, providing a higher number of secondary reactions of poly condensation and obtaining materials with high homogeneity and a more reduced surface area, as observed for sample A2 [27,28].

The experimental pore diameter value obtained for the sample A1 (42.07 Å) is very close to the calculated one (41.25 Å). For the A2 sample, the values are not close (90.03 versus 110.90 Å), and this difference can be attributed to a deviation from a perfect cylindrical geometry of the pores, as assumed by the Barrett, Joyner, and Halenda (BJH) model. The N_2 adsorption isotherms obtained from the samples correspond to the type IV isotherm (Figure 1), indicating that

the materials are mesoporous, with pore diameters within the range 20-500 Å.

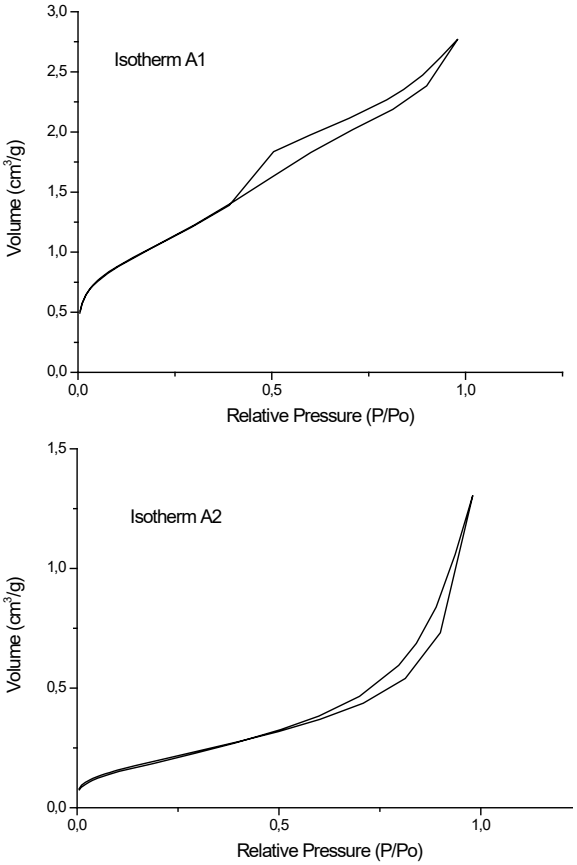

Figure 1. N_2 adsorption isotherms of the prepared sol-gel glasses A1 and A1.

The thermal behavior of the samples is presented in Figure 2. In the TGA plot, there are three weight loss regions and the mass is lost up to 770°C and 710 °C for A1 and A2 samples, respectively, after that no more significant variations occurred.

According to Figure 2, regarding the A1 sample, the first weight loss region (between 60 °C and 184 °C), is related to the endothermic process of desorption of physically adsorbed water and alcohol [17,29]. In the second region (between 184 °C and 483 °C), the weight loss is related to the release of chemically adsorbed water and ethanol [29]. The third region, which occurs between 483°C and 770 °C, is due to the burning out of the organic compounds resulting from the incomplete condensation of the precursors, and to the elimination of nitrate ions present in the precursor salts used in the gel preparation [29]. As indicated by the level in the TGA plot (beyond ≈770 °C), there was no further significant weight loss, and its total value was approximately 40%. The thermal behavior of sample A2 is similar to the one observed for sample A1. However, the first weight loss region is observed between 57°C and 147°C; the second between 147 °C and 471 °C and the third between 471 °C and 710 °C. The weight loss stops at a slightly lower temperature (≈710 °C), and the total weight loss is also reduced (33%). The observed difference in the thermal behavior of the samples is a consequence of the synthesis process used to prepare the powders. In the first case, the precursors are in distinct phases, a solid and a liquid, and in the A2 composition all the precursors are liquid, which provides a more effective mixture and network formation [29].

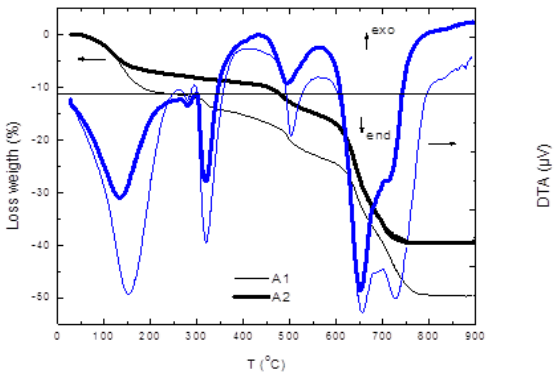

Figure 2. DTA and TGA curves of A1 and A2 samples.

These results suggest that the TiO_2 precursor has a strong influence on the type of the crystalline phases formed, which can be associated with the homogeneity degree of the primary mixture. The X-ray patterns of the obtained powders, in Figure 3, show the presence of some crystalline phases before heating and after the thermal treatment at 600°C, 800 °C, and 900°C. The temperature of 600ºC was used for the nitrate elimination of the samples, and the temperatures of 800ºC and 900ºC were chosen for the thermal stability of samples A1 and A2.

The sample A1 exhibits, before the thermal treatment, three crystalline phases: sodium nitrate (cod.01-089-0311), titanium oxide (anatase) (cod. 01-073-1764) and calcium phosphate hydroxide (cod. 00-009-0080) [30]. In the sample A2, only one crystalline phase - sodium nitrate (cod.01-089-0311) was identified. When the samples are treated at different temperatures, the occurrence of new crystalline phases (cod. 01-084-0196, cod.

01-076-1456, cod. 01-070-0360, cod. 01-089-8960 and cod.01-089-6439) arises, what is more evident for A1 than A2. An approximate calculation of the volume % of crystalline phases in the samples [30] indicated that, after the thermal treatment at 900°C, the crystallinity degree observed was 48% for A1 and 36% for A2.

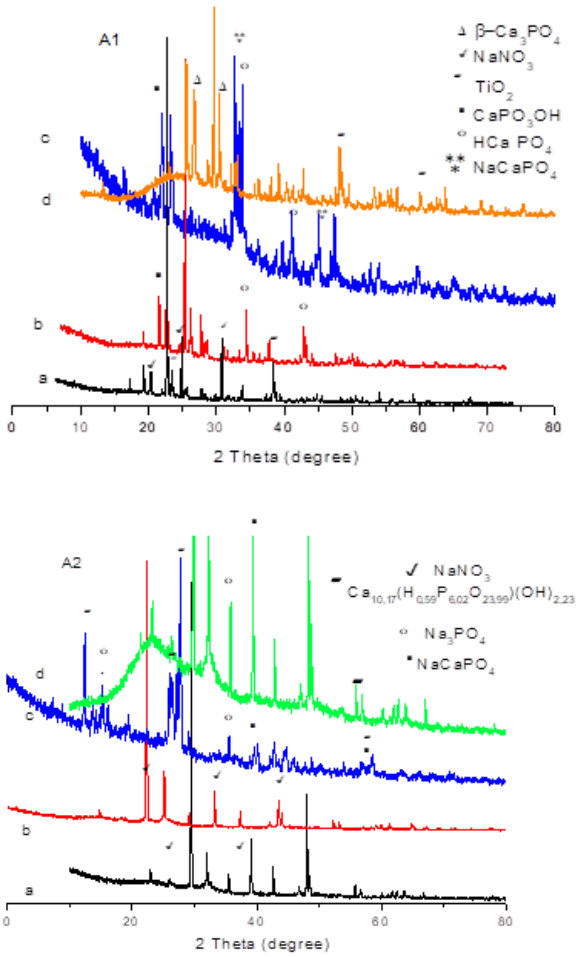

Figure 3. X-ray diffraction patterns of the samples A1 and A2: (a) before heating; after the thermal treatment at (b) T= 600 °C for 3 hours, (c) T= 800 °C for 3 hours and (d) T= 900 °C for 3 hours.

In the case of the A1 composition, the initial mixture is more heterogeneous due to the solid TiO_2, whereas for the A2 sample the starting reaction medium is homogeneous since TTP is liquid. The influence of metallic oxides in the glass network formation has been reported by several authors. The addition of titanium oxide to a glass shows a decrease in Tg related to a depolymerization of the vitreous network and the formation of Si-O-Ti. In the case of the sample A1, the fact that the titanium oxide is not in the same phase of the other reactants hampers the interaction between Ti and Si at the atomic level and the occurrence of new crystalline phases containing both ions [11,24,31,32]. When the samples are treated at different temperatures (Figure 3), new crystalline phases arise, which are more evident for A1 than A2. Again, the influence of the titanium oxide precursor is observed.

The FT-IR spectra of the samples A1 and A2 are presented in Figure 4, and the assignments of the respective bands are shown in Table 2. Very similar profiles between the samples A1 and A2 are verified, but particular attention should be taken to the band in the region 1380cm^{-1}. In this region, a clear change in the intensity of the band is observed for the samples A1 and A2 when submitted to the heat treatment and in the presence of an acid medium.

The bands around 1050 -1100 cm^{-1} are related to the asymmetric stretches of the Si-O-Si in the SiO_4 tetrahedral unit. The presence of a strong and broad band in this region indicates the presence of the SiO_4 structural units [32–37]. The bands around 830 cm^{-1} and a band, of medium intensity, at 630 cm^{-1} are due to the Ti-O stretching and indicate the Ti-O connections from tetrahedral TiO_4 [22,37]. The weak bands between 400 and 480 cm^{-1} can be associated with the angular deformation of Ti-O-Ti or Ti-O-Si bonds. The bands between 900 and 980 cm^{-1} are attributed to the Si-OH groups. When the structural units SiO_4 are completely polymerized (Q^4, Si-O-BO), a band at 1200 cm^{-1} appears. However, in the spectra of samples A1 and A2 this band is shifted to the region between 1175 and 1100 cm^{-1}. This indicates the depolymerization of the silicate networks (Q^3 Si-O-NBO) due to the addition of TiO_2, and it can provide changes in the connectivity of the networks [38–41]. The presence of the band in the region between 900-960 cm^{-1} is indicative of the Si-O-Ti bond [42]. It indicates that the Ti acts predominantly as a network modifier [34]. Some authors attribute the Ti presence to the depolymerization process of the silicate glass network, resulting in a higher concentration of Si–NBO bonds and enhancing the degradability of the glass [39,43–45]. The weak bands between 400 and 480 cm^{-1} can be related to the angular deformation of Ti-O-Ti or Ti-O-Si bonds. The bands between 900 and 980 cm^{-1} are attributed to the Si-OH groups.

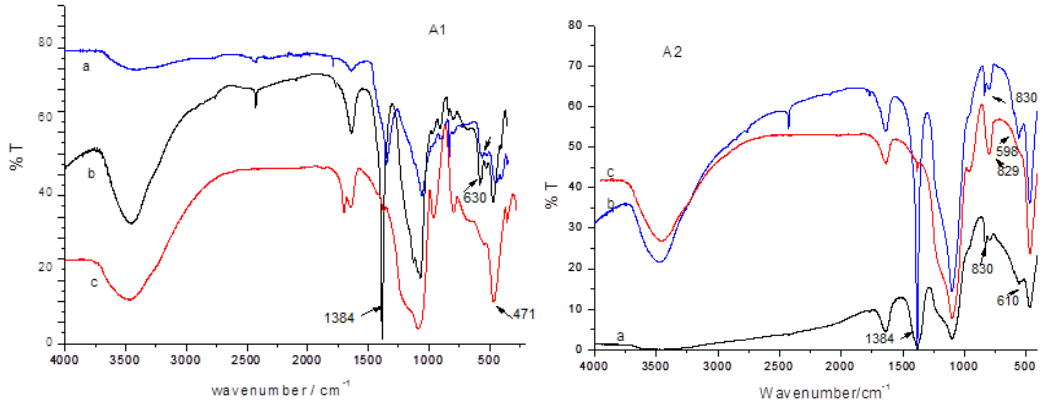

Figure 4. ATR-IR spectra for A1 sample; a) prepared; b) after the heat treatment at 600ºC, 3 hours and c) after the heat treatment at T = 600ºC and acid attack with HCl 1 M, 1 hour. A2 sample a) prepared; b) after the heat treatment at 600ºC, 3 hours and c) after the heat treatment at T = 600ºC and acid attack with HCl 1 M, 1 hour.

Table 2. Absorption bands observed in the FT-IR spectra (KBr pellets), ATR-IR and Raman (powders).

	Wave number (cm^{-1})			Attribution
Sample	**FT-IR**	**ATR-IR**	**Raman**	
A1	3474(w)	3417(w)	3431(m)	ν_{O-H}
	2427(vw)	2426(w)	-	ν_{C-H}
	1770(vw)	1789(w)	-	ν_{C-O}
	1635(s)	1637(w)	1669(m)	ν_{C-O-O^-}
	1384(s)	1351(w)	1384(w)	ν_{NO3^-}
	1175(sh)	-	-	ν_{Si-O}
	1130(w)	1100(sh)	-	ν_{Si-O}
	1070(vw)	1058(s)	1067(s)	$\nu_{Si-O-Si}$
	-	-	1051(w)	$\nu_{Si-O-Si}$
	973(w)	940(sh)	982(w)	ν_{Si-O}
	915(vw)	900(w)	-	ν_{Si-O}
	829(w)	834(s)	-	ν_{Ti-O}(Td)
	-	726(vw)	724(w)	$\nu_{Si-O-Si}$ (Td)
	-	-	637(m)	ν_{Ti-O}(Td)
	580(w)	-	-	ν_{P-O} (amorphous)
	566(sh)	560(w)	-	ν_{P-O} (amorphous)
	525(vw)	520(vw)	514(w)	ν_{P-O} (crystalline)
	471(w)	448(w)	-	$\nu_{Ti-O-Ti}$
		401(vw)	395(w)	ν_{Ti-O}(Td)
			186(m)	ν_{Ti-O}(Td and Oh)
			142(s)	ν_{Ti-O}, TiO_2(anatase)
A2	3450(w)	3371(w)	-	ν_{O-H}
	2427(vw)	2430(w)	-	ν_{C-H}
	1763(vw)	1789(w)	-	ν_{C-O}
	1637(s)	1637(m)	1669(vw)	ν_{C-O}
	1384(s)	1353(s)	1384(m)	ν_{NO3^-}
	1103(s)	1048(s)	1067(s)	$\nu_{Si-O-Si}$
	829(m)	834(m)	959(w)	ν_{Si-O}, ν_{Ti-O}
	796(w)	796(w)	-	ν_{Ti-O} (Td)
	-	725(vw)	724(m)	$\nu_{Si-O-Si}$ (Td)
	600(vw)	598(vw)	682(vw)	ν_{Ti-O} (Td)
	559(w)	554(vw)	-	ν_{P-O} (amorphous)
	471(s)	446(s)	425(w)	$\nu_{Ti-O-Ti}$
			186(s)	ν_{Ti-O} (Td and Oh)

s: strong; m: medium, w: weak, vw: very weak; sh: shoulder.

The ATR-IR spectra of samples A1 and A2 heated at 600 °C for 3 h, before and after the treatment with HCl 1 mol L^{-1}, are shown in Figure 4. The band at 1384 cm^{-1} presented in the IR spectra of these samples is frequently attributed to the presence of the vibrational modes of the NO_3^- group. The objective of the heat treatment at 600°C was to eliminate the NO_3^- ions from the samples. Nevertheless, this band exhibited an

intensification and became sharper after the heat treatment at 600ºC. This band almost disappeared after the contact with the HCl solution. A similar behavior is observed for the band around 830-840 cm^{-1}. In this context, some authors attribute the bands at 1384 cm^{-1} and 830-840 cm^{-1} to the stretching of the groups CO_3^{2-} and HCO_3^-, respectively [46–48]. The absence of these bands, after the contact with the acidic solution, indicates the elimination of the CO_3^{2-} and HCO_3^- ions by the acid reaction. It is possible that their incorporation occurred during the powder synthesis resulting from the decomposition of the organic part of the reactants used.

The infrared spectra of the powder samples after forming the glass ionomer cements are presented in Figure 5, and the corresponding bands are shown in Table 3. In these FTIR spectra, we should emphasize the bands around 1700cm^{-1}, 1500cm^{-1}, and 800cm^{-1} that changed the profile and presented some shift in the position.

Table 3. Absorption bands of the FT-IR spectra for the commercial cements and for the synthesized powder ionomer cements. Groups identified in Table 4.

	Cements Group					
	I	**II**	**III**	**IV**	**V**	**VI**
Wavenumber (cm^{-1})	3458(m)	3440(s)	3433(s)	3200(m)	3390(m)	3392(m)
	2964(w)				2931(w)	2940(w)
				1981(w)		
			1869(vw)			
	1717(m)				1701(s)	1701(s)
	1635(w)	1696(w)	1697(vw)	1684(s)		
	1601(vw)	1624(s)				
			1589(s)			
	1457(m)			1449(w*)	1449(m*)	1449(m*)
	1413(w)				1413(m*)	1412(m*)
		1384(m)	1384(s)	1392(w*)		
		1333(w)				
	1169(w)		1104(s)	1161(vw)		
	1081(m)	1092(s) 960(m)		1059(m)	1062(m)	1064(m)
	970(w)	813(m*)	962(w)	952(vw)	955(w*)	957(w)
		793(m*)	815(m)			
				796(vw)	790(w*)	790(m*)
			711(m)			
	645(w)	565(w) 532(w)			667(w)	668(w)
		469(s)				659(vw)
			534(w)			
			472(s)			
	449(m)				444(m*)	453(m)

Band intensity: s=strong; m=medium, w=weak, vw=very weak; sh=shoulder; m*=medium to weak; w*= weak to very weak.

According to Figure 5, it can be observed a similarity between the profiles of the spectra obtained from the samples of commercial glass ionomer cements (groups I and IV, Table 4) and the prepared powders ionomer cements (groups II, III, V and VI). Comparing the data presented in Tables 2 and 3 and the spectra in Figure 5, it was observed that the weak intensity bands at 1770 cm^{-1} (sample A1) and 1763 cm^{-1} (sample A2) disappeared after the cement formation. Similarly, the strong band at 1384 cm^{-1} shows an intensity reduction after the reaction of the powders with the polymeric acid solutions. It was also observed the occurrence of weak intensity bands at 1457 cm^{-1} and an increase of the intensity of the band around 800 cm^{-1}. These bands are attributed to the CO_3^{2-} group that appears after the reaction with the organic acid [49–51]. The neutralization reaction of the organic acid is mainly characterized by the absence of the band around 1750 cm^{-1} assigned to C-O and C=O of the poly acid. The band at 1460 cm^{-1} can be related to the

symmetric and asymmetric COO^- stretch, and the band around 1380 cm^{-1} is attributed to the symmetric stretch in poly acid salts. In contrast, the band at 580 cm^{-1} increases after the reaction with the organic acids. This band indicates the presence of CO_3^{2-} groups that occupy the place of the trivalent phosphate ions (PO_4^{3-}) in the material structure [49,52,53]. This behavior confirms the reaction between the particles of the powder glass and the poly organic acid solutions used to obtain the cements.

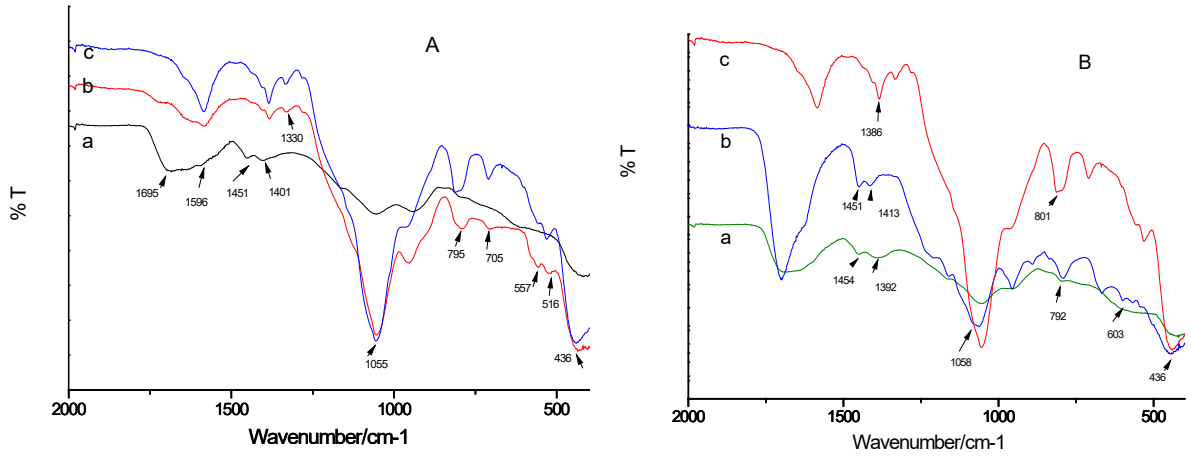

Figure 5. FTIR spectra of powder ionomer cements: A- a) Group I, b) Group II, c) Group III; B- a) Group IV, b) Group V, c) group VI. Groups identified in Table 1.

3. Material and Methods

Powder Synthesis

Powders with the composition $47SiO_2$-$13CaO$-$29Na_2O$-$7P_2O_5$-$4TiO_2$ (mole %) were synthesized by the sol-gel method. The raw materials used were phosphoric acid, H_3PO_4 (85%, Aldrich), sodium nitrate, $NaNO_3$ (99%, Sigma-Aldrich), calcium nitrate tetrahydrate, $Ca(NO_3)_2.4H_2O$ (99%, Sigma-Aldrich), and tetraethyl orthosilicate (TEOS, 99% Aldrich). The source of titanium was titanium oxide, TiO_2 (99,99%, Aldrich) (composition A1) and titanium tetraisopropoxide (TTP, Aldrich) (composition A2).

Initially, the hydrolysis of TEOS was catalyzed with a solution of 0.1mol L^{-1} HNO_3, in the presence of ethanol under continuous stirring in an open vessel at room temperature for 60 minutes. A second solution was prepared dissolving sodium and calcium nitrate in distilled water. This solution was added dropwise to the hydrolyzed TEOS solution. The titanium oxide (for A1) or the titanium tetraisopropoxide (for A2) were then added, and the mixture was kept under constant stirring for 60 minutes. Jellification was achieved after one week aging the mixture. After that time, the gels were dried for one week at 60 °C and three days at 120 °C. Both compositions resulted in powders that were ground in an agate mortar and further characterized.

Cement Preparation

Powders of both compositions A1 and A2 were sieved (75 μm) and then used to produce the cements. For comparison purposes, two commercial powders named Vidrion C® Cementation and Maxion® R Restorative were used to prepare ionomer cements with the powder/liquid ratios 1:1 as indicated by the manufacturer. The luting pastes prepared with the synthesized powder ionomers were obtained at room temperature by hand mixing the powder and the liquid components according to the weight ratios indicated in Table 4. Table 4 shows the composition of the six groups of cements, where those identified as I, II and III refer to the situations in which the liquid phase used to obtain the experimental cements (II and III) was the same used for the commercial group I, Vidrion C® Cementation. In the case of the groups IV, V and VI, the liquid phase for the experimental cements V and VI was the one used for the commercial cement Maxion®R Restorative, group IV.

Table 4. Composition of the powder ionomer cements (synthesized and commercial) and powder liquid ratio. Groups designation in the first column makes reference to the nature of the powder and the liquid in the composition.

Group	Powder	Powder:Liquid ratio (w/w)	Composition
I	Vidrion C® Cementation Lot number:0061112	P/L= 3.0	Powder: Ca-Al-F silicate glass, polyacrylic acid. Liquid: tartaric acid, distilled water.
II	A1	P/L= 2.0	Powder: Ca-Na-P-Ti silicate glass Liquid: tartaric acid, distilled water.
III	A2	P/L= 0.7	Powder: Ca-Na-P-Ti silicate glass Liquid: tartaric acid, distilled water.
IV	Maxxion R® Restorative Lot number: 010513	P/L= 1.3	Powder: Al-F silicate glass. Liquid: polyacrylic acid, tartaric acid, calcium fluorite and distilled water.
V	A1	P/L= 1.3	Powder: Ca-Na-P-Ti silicate glass Liquid: polyacrylic acid, tartaric acid, calcium fluorite and distilled water.
VI	A2	P/L= 0.7	Powder: Ca-Na-P-Ti silicate glass Liquid: polyacrylic acid, tartaric acid, calcium fluorite and distilled water.

4. Conclusions

In this study, powders ionomer cements with the composition $47SiO_2$-$13CaO$-$29Na_2O$-$7P_2O_5$-$4TiO_2$ were synthesized by the sol-gel method at 600ºC using two alternative TiO_2 sources. The specific surface areas of the obtained powders were higher than those of the commercial ionomers.

The TiO_2 source (titanium oxide or titanium tetraisopropoxide, TTP) demonstrated a strong influence on the powder thermal behavior and the crystallization process. A high crystallinity was observed in both powders, and the one prepared from the TiO_2 powder (A1) showed distinct crystalline phases compared to the powder prepared with titanium tetraisopropoxide (A2). Both powders A1 and A2 presented high thermal stabilities.

The FTIR spectra exhibited the interaction between the powder and the polymeric acid solution, showing the feasibility of the prepared powders to be used in the preparation of ionomer cements, following the same procedure established for the commercial ionomer glasses.

These materials have promising characteristics for biomedical applications, particularly for dental restoration.

Acknowledgments

The authors acknowledge the financial support from CICECO (**Pest-C/CTM/LA0011/2013)**, FEDER, QREN, COMPETE and FCT. Thanks also to the State University of West Paraná.

References and Notes

[1] Castillo-Oyagüe, R.; Lynch, C. D.; Turrión, A. S.; López-Lozano, J. F.; Torres-Lagares, D.; Suárez-García, M. J. *J. Dent*. **2013**, *41*, 90. [Crossref]

[2] Silva, R. M.; Santos, P. H. N.; Souza, L. B. ; Dumont, V. C. ; Soares, J. A.; Santos, M. H. *Mater. Res. Bull.* **2013**, *48*,118. [Crossref]

[3] Nicholson, J. W. *Biomaterials,* **1998**, 485. [Crossref]

[4] Akinmade, A. O.; Nicholson, J. W. *J. Mater. Sci. Mater. Med.* **1993,** *4*, 219. [Crossref[

[5] Brook, I. M.; Hatton, P. V. *Biomaterials,* **1998**, 565. [Crossref]

[6] Hatton, P. V.; Hurrell-Gillingham, K. ; Brook, I.M. *J. Dent.* **2006,** *34*, 598. [Crossref]

[7] Boyd, D. ; Towler, M. R.; Wren, A.; Clarkin, O. M. *J. Mater. Sci. Mater. Med.,* **2008**, 1745. [Crossref]

[8] Dos Santos, R. L. ; Pithon, M.M. ; Martins, F. O.; Romanos, M. T. V.; Ruellas, A. C. O.*Eur. J. Orthod*. **2012**, *34*, 362. [Crossref]

[9] Nicholson, J. W. ; Braybrook, J. H.; Wasson, E. A. *J. Biomater. Sci. Polym*. **1991,** 277. [Crossref]

[10] Majekodunmi, A. O.; Deb, S. *J. Mater. Sci. Mater. Med.* **2007**, *18*, 1883. [Crossref]

[11] Nourmohammadi, J.; Sadrnezhaad, S. K. ; Behnam Ghader, A. *J. Mater. Sci. Mater. Med.* **2008,** *19*, 3507. [Crossref]

[12] Brito, C. R.; Velasco, L. G.; Bonini, G. A. V. C.; Imparato, C. P.; Raggio, P.; Imparato, J. C. P.; Raggio, D. P. *J. Biomed. Mater. Res. - Part A.* **2010,** *93*, 243. [Crossref]

[13] Wood, D.; Hill, R. *Biomaterials.* **1991,** *12*, 164. [Crossref]

[14] Clifford, A.; Hill, R. *J. Non. Cryst. Solids.* **1996,** *196*, 346. [Crossref]

[15] Kim, Y. S. Tressler, R. E. *J. Mater. Sci.* **1994,** *29*, 2531. [Crossref]

[16] Balamurugan, A.; Sockalingum, G.; Michel, J.; Fauré, J ; Banchet, V.; Wortham, L.; Bouthors, S.; Laurent-Maquin, D.; Balossier, G. *Mater. Lett.* **2006**, *60*, 3752. [Crossref]

[17] Siqueira, R. L.; Peitl, O.; Zanotto, E. D. *Mater. Sci. Eng. C.* **2011,** *31*, 983. [Crossref]

[18] Balamurugan, A.; Balossier, G.; Laurent-Maquin, D.; Pina, S.; Rebelo, A. H. S. ; Faure, J.; Ferreira, J. M. F. *Dent. Mater.* **2008,** *24*, 1343. [Crossref]

[19] Epiphanova, A.; Magaev, O.; Vodyankina, O. *J. Sol-Gel Sci. Technol.* **2012,** *61*, 509. [Crossref]

[20] Fathi, M. H.; Hanifi, A. *Mater. Lett.* **2007,** *61*, 3978. [Crossref]

[21] Bertolini, M. J.; Zaghete, M. A.; Gimenes, R.; De Souza, R. F.; Vaz, L. G. J. *Non. Cryst. Solids.* **2004,** *344*, 170. [Crossref]

[22] Li, P.; Ohtsuki, C.; Kokubo, T.; Nakanishi, K.; Soga, N.; de Groot, K. *J. Biomed. Mater. Res.* **1994,** *28*, 7. [Crossref]

[23] Jevnikar, P.; Golobič, M.; Kocjan, A.; Kosmač, T. *J. Eur. Ceram. Soc.* **2012,** *32*, 2641. [Crossref]

[24] Abo-Mosallam, H. A.; Park, H. C. *Mater. Lett.* **2012,** *72*, 137. [Crossref]

[25] Moshaverinia, A.; Roohpour, N.; Chee, W. W. L.; Schricker, S. R. *J. Mater. Chem.* **2012,** *22*, 2824. [Crossref]

[26] Gallinetti, S.; Canal, C.; Ginebra, M.-P.; Ferreira, J. *J. Am. Ceram. Soc.* **2014,** *97*, 1065. [Crossref]

[27] Krivtsov, I. V.; Ilkaeva, M. V.; Avdin, V. V.; Zherebtsov, D. A. *J. Non. Cryst. Solids.* **2013,** *362*, 95. [Crossref]

[28] Laczka, M.; Cholewa-Kowalska, M. K.; Laczka-Osyczka, A.; Turyna, B. *J. Biomed. Mater. Res.* **2000,** *52*, 601. [Crossref]

[29] Izquierdo-Barba, I. ; Salinas, A. J. ; Vallet-Regí, M. *J. Biomed. Mater. Res.* **1999,** *47*, 243. [Crossref]

[30] Wong-Ng, W.; Snyder, R. L.; Park, C.; Antipov, E.; McClune, W. F. *Powder Diffr.* **1997,** 12. [Crossref]

[31] Mezahi, F. Z.; Girot, A. L.; Oudadesse, H.; Harabi, A. *J. Non. Cryst. Solids.* **2013,** *361*, 111. [Crossref]

[32] Sung, Y. M.; Dunn, S. A. ; Koutsky, J. A. *J. Eur. Ceram. Soc.* **1994,** *14*, 455. [Crossref]

[33] Park, J.; Ozturk, A. *Thermochim. Acta.* **2008**, *470*, 60. [Crossref]

[34] Wren, A.; Clarkin, O. M.; Laffir, F. R.; Ohtsuki, C.; Kim, I. Y; Towler, M. R. *J. Mater. Sci. Mater. Med.* **2009,** *20*, 1991. [Crossref]

[35] Wren, A. W.; Kidari, A.; Cummins, N. M.; Towler, M. R. *J. Mater. Sci. Mater. Med.* **2010,** 1. [Crossref]

[36] Naumenko, A.; Gnatiuk, I.; Smirnova, N.; Eremenko, A. *Thin Solid Films*, **2012**, 4541. [Crossref]

[37] Crisp, S.; Pringuer, M. A.; Wardleworth, D.; Wilson, A. D. *J. Dent. Res.* **1974,** *53*, 1414. [Crossref]

[38] Dutoit, D. C. M.; Schneider, M.; Baiker, A. *J. Catal.* **1995,** *153*, 165. [Crossref]

[39] Klein, S.; Thorimbert, S.; Maier, W.F. *J. Catal.* **1996,** *163*, 476. [Crossref]

[40] Yatongchai, C. ; Placek, L. M.; Curran, D. J.; Towler, M. R.; Wren, A. W. J. *Biomater. Appl.* **2015,** 1. [Crossref]

[41] Sauro, S. ; Watson, T. F.; Thompson, I.; Toledano, M.; Nucci, C.; Banerjee, A. *Eur. J. Oral Sci.* **2012,** *120*, 168. [Crossref]

[42] Gao, X.; Wachs, I.E. *Catal. Today* **1999,** *51*, 233. [Crossref]

[43] Laiteerapong, A.; Lochaiwatana, Y.; Hirata, I. ; Okazaki, M.; Mori, K.; Murakami, S.; Poolthong, S. *Dent. Mater.* J. **2012,** *31*, 772. [Crossref]

[44] Wren, A. W.; Coughlan, A.; Placek, L.; Towler, M. R. *J. Mater. Sci. Mater. Med.* **2012,** *23*, 1823. [Crossref]

[45] Hashimoto, M.; Iijima, M.; Nagano, F. ; Ohno, H.; Endo, K. *J. Biomed. Mater. Res. - Part B Appl. Biomater.* **2010,** *94*, 127. [Crossref]

[46] Soares, P.; Laurindo, C. A. .; Torres, R. D.; Kuromoto, N. K.; Peitl, O.; Zanotto, E. D. *Surf. Coatings Technol.* **2012,** *206*, 4601. [Crossref]

[47] Mansur, H. S.; Costa, H. S. ; Mansur, A. A. P.; Pereira, M. *Mater. Sci. Eng. C.* **2012,** *32*, 404. [Crossref]

[48] Diba, M.; Fathi, M. H.; Kharaziha, M. *Mater. Lett.* **2011,** *65*, 1931. [Crossref]

[49] Gomes, F. O. ; Pires, R. A. ; Reis, R.L. *Mater. Sci. Eng. C.* **2013,** *33*, 1361. [Crossref]

[50] Sauro, S.; Osorio, R.; Fulgencio, R.; Watson, T. F.; Cama, G.; Thompson, I.; Toledano, M. *J. Mater. Chem. B.* **2013,** *1*, 2624. [Crossref]

[51] van der Houwen, J. A. M.; Cressey, G.; Cressey, B. A.; Valsami-Jones, E. *J. Cryst. Growth.* **2003,** *249*, 572. [Crossref]

[52] Radev, L.; Hristov, V.; Michailova, I.; Samuneva, B. *Open Chem.* **2009,** *7*, 322. [Crossref]

[53] Wren, A. W.; Hansen, J. P.; Hayakawa, S.; Towler, M. R. *J. Mater. Sci. Mater. Med.* **2013,** *24*, 1167. [Crossref]